A Numerical Investigation on Residual Energy of Labyrinth Weirs

P. Langohr
FH Aachen University of Applied Sciences, langohr@fh-aachen.de

B. M. Crookston
Utah State University, brian.crookston@usu.edu

D. B. Bung
FH Aachen University of Applied Sciences

Recommended Citation

Langohr P., Crookston, B.M., and Bung, D.B. (2022). "A Numerical Investigation on Residual Energy of Labyrinth Weirs" in "9th IAHR International Symposium on Hydraulic Structures (9th ISHS)". *Proceedings of the 9th IAHR International Symposium on Hydraulic Structures – 9th ISHS*, 24-27 October 2022, IIT Roorkee, Roorkee, India. Palermo, Ahmad, Crookston, and Erpicum Editors. Utah State University, Logan, Utah, USA, 8 pages (DOI: 10.26077/fdab-c7cd) (ISBN 978-1-958416-07-5).

9th International Symposium on Hydraulic Structures Roorkee, India 24-27 October 2022
ISBN 978-1-958416-07-5 DOI: https://doi.org/10.26077/fdab-c7cd

A Numerical Investigation on Residual Energy of Labyrinth Weirs

P. Langohr[1], B.M. Crookston[2] & D.B. Bung[1]
[1]*FH Aachen University of Applied Sciences, Aachen, Germany*
[2]*Utah Water Research Laboratory, Utah State University, Logan (UT), USA*
E-mail: langohr@fh-aachen.de

Abstract: *The replacement of existing classical weirs with labyrinth weirs is a proven techno-economical solution and a means to increase the discharge capacity when rehabilitating existing structures. However, flows exiting a labyrinth weir are complex, three-dimensional, and aerated; additional information is needed regarding energy dissipated by such weirs. In this study, three labyrinth weirs with different crest lengths were simulated with FLOW-3D HYDRO. Reynolds-averaged Navier-Stokes (RANS) modeling with the use of finite-volume method and Re-Normalisation Group (RNG) k-ε turbulence closure were employed. An attempt was made to more precisely account for the flow field in the downstream region. Consequently, the velocity head was determined with both depth-averaged and section-averaged velocities. Additionally, the kinetic energy correction coefficient was considered. A comparison of the computational fluid dynamics (CFD) results with prior experimental data showed that the residual energy was influenced by factors such as probe position and geometric parameters. A minor influence was observed for the kinetic energy correction coefficient. Overall, the high amount of energy dissipation was underlined and an acceptable agreement between simulated and literature data was documented.*

Keywords: *CFD, energy dissipation, labyrinth weirs*

1. Introduction

Due to the aging of existing hydraulic structures and increased societal demands, rehabilitation techniques have gained importance. Deficiencies to be addressed by rehabilitation include not only hydraulic and structural issues, but also factors such as climate change, longer hydrologic records, and urbanization. Replacing classical, linear weirs with nonlinear weirs (e.g., labyrinth weir, piano key weir) is one possibility to increase the discharge capacity of an existing spillway while construction costs and space requirements may impede the widening of existing linear weirs. Regarding the number of published articles in scientific journals and realized prototypes, a continuous increase of interest in this type of hydraulic structure is eminent (Crookston et al. 2019; Hager et al. 2015; Schleiss 2011). Another positive aspect of nonlinear weirs is the wide range of application from river structures to flood protection spillways.

In general, nonlinear weirs are characterized by repetitive cycles in plan view (Fig. 1). Since their introduction, numerous design approaches (Erpicum et al. 2017; Erpicum et al. 2013; Erpicum et al. 2011; Crookston 2010; Falvey 2003; Hinchliff and Houston 1984; Hay and Taylor 1970; Taylor 1968) as well as innovative design ideas (Ben Said and Ouamane 2022; Akbari Kheir-Abadi et al. 2020; Ghaderi et al. 2020; Bilhan et al. 2018; Dabling and Tullis 2017; Crookston and Tullis 2012; Dabling and Crookston 2012) have been proposed. Possible cycle shapes are rectangular (A), trapezoidal (B) or triangular (C) (see Fig. 1) with trapezoidal most common. Generally, these weirs cause a three-dimensional flow field immediately downstream and such turbulence provides energy dissipation. Particularly downstream of the weir, significant free-surface fluctuations are encountered. Therefore, collection of relevant hydraulic parameters in the laboratory is challenging. To date, there is still limited information about the energy dissipation processes and their dependence on selected geometric parameters (Carrillo et al. 2020; Crookston 2020; Merkel et al. 2018; Lopes et al. 2011, 2008, 2006; Magalhaes and Lorena 1994). Specifically, how does a labyrinth weir influence the design of a stilling basin in a rehabilitation project? Therefore, in this study numerical simulations were conducted of quarter-round trapezoidal labyrinth weirs with varying cycle lengths to estimate the relative residual energy and study the influence of parameters such as probe position and different velocity head determination methods.

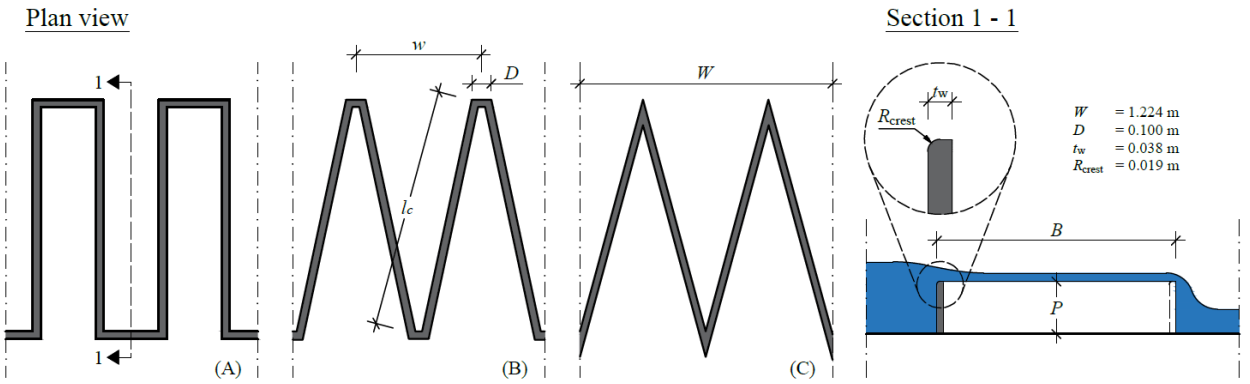

Figure 1. Plan view of typical nonlinear weir cycle shapes (rectangular (A), trapezoidal (B) or triangular (C))

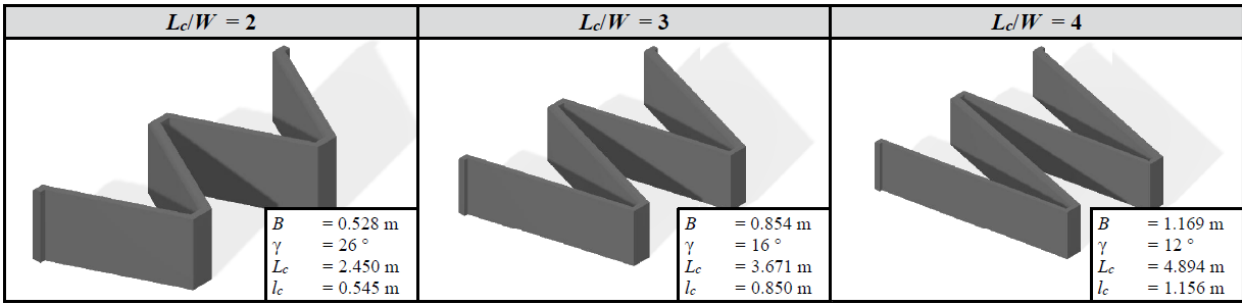

Figure 2. Geometries of the studied labyrinth weirs.

2. Numerical Model

2.1. Overview

Three different quarter-round trapezoidal labyrinth weirs were investigated. With a constant weir height of $P = 30.5$ cm and a total flume width of $W = 1.22$ m, only the ratio of total crest length to total width (L_c/W) is varied from 2 to 4. According to this increase of L_c/W, the corresponding sidewall angles γ were 26°, 16° and 12° (see Fig. 2). For each geometry a total of 5 discharges with $0.05 < Q \leq 0.25$ m³/s were investigated. Along the computational domain, several numerical probes for data extraction were considered placed in three transects each centered on an upstream labyrinth apex. The selected labyrinth weir dimensions were of laboratory scale model and were similar to published geometries by Crookston (2020, 2010) and Tullis et al. (2020; 2005).

2.2. Numerical Settings

For this study, the three-dimensional Reynolds-averaged Navier-Stokes (RANS) equations were solved by FLOW-3D HYDRO using a finite-volume method (Hirt and Nichols 1981) and Re-Normalisation Group (RNG) *k-ε* (Yakhot et al. 1992) turbulence closure with dynamically computed characteristic turbulence length. Further details of the numerical methods are described i.e. by Versteeg and Malalasekera (2007) or Wilcox (2006). The single fluid approach of FLOW-3D was chosen for this study (Crookston et al. 2018; Mansoori et al. 2017; Bayon et al. 2016). According to Flow Science, Inc. (2020) all values, except fractional areas and velocities, are computed at the center of each cell. The remaining values are calculated in the center of the hexahedral cell faces.

To minimize computation time, a nested multiblock mesh with varying cell sizes was used in this study (see. Fig. 3). The finest mesh resolution was considered for the vicinity of the structure. Referring to the upstream labyrinth weir face, the inlet and outlet boundaries were located 3 m upstream and 5.5 m downstream. A volume flow rate was defined as an upstream boundary condition (BC). The downstream BC was defined as a water surface elevation equal to zero. Both vertical sides as well as the horizontal floor were defined as smooth walls.

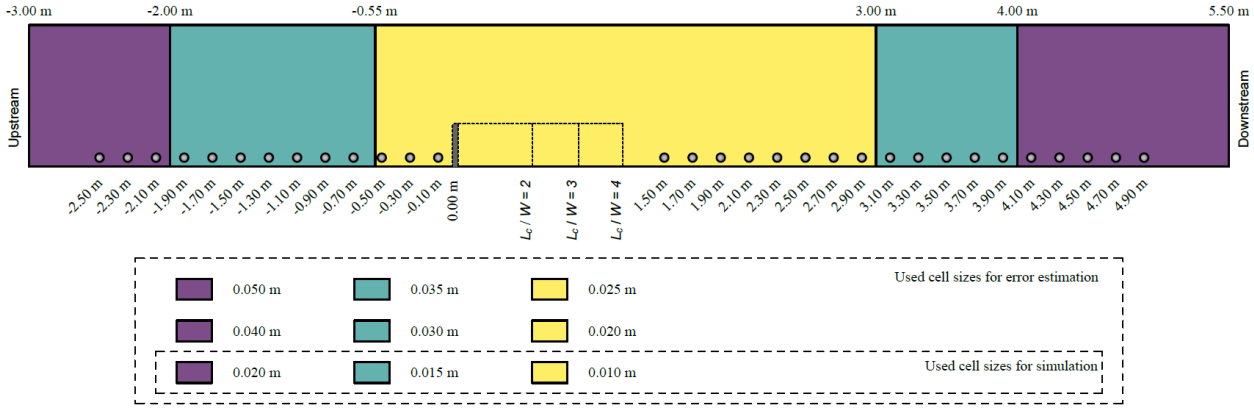

Figure 3. Sideview of the numerical domain, considered cell sizes for the nested multi-block mesh and location of numerical probes for error estimation and data analysis.

A mesh sensitivity analysis was conducted considering the grid convergence index (GCI; Roache 1994) and the methodology as proposed by Celik et al. (2008). Accordingly, three different representative cell sizes were assessed for each mesh (see Fig. 3). For verification, two geometries and discharges ($L_c/W = 2$ with $Q = 0.05$ m^3/s; $L_c/W = 4$ with $Q = 0.25$ m^3/s) were used. For both analyses, six GCI values (3 upstream, 3 downstream) for flow depth h, depth-averaged velocity U_{DA} and Froude number F_r were calculated. This results in a total of 36 GCI values with a mean GCI of 9.2 %. As expected, the GCI values are higher for low discharges and downstream of the weir. This may be caused by an increased inaccuracy of the volume of fluid method at low water levels downstream of the weir. An opposite trend is documented for higher discharges at the upstream area. The used mesh sizes were in a comparable size to several published studies (Ben Said and Ouamane 2022; Carrillo et al. 2020; Ghaderi et al. 2020; Carrillo et al. 2019; Crookston et al. 2018). As a result, the sensitivity analysis shows adequate values. With the used mesh sizes, each simulation required between three to seven days using a 8-core Intel(R) Xeon(R) CPU at 2.10GHz.

3. Results

3.1. Flow Depth

Resulting water levels from all configurations are illustrated in Figure 4. Downstream of the weir, no classic hydraulic jump was observed. The results show more of a plunging jet into the downstream water body. Air entrainment is disregarded in the employed single fluid approach; a related subgrid model was not activated. However, Valero et al. (2018) showed that energy dissipation processes at hydraulic structures can be modeled with reasonable accuracy neglecting air entrainment. Due to high-turbulence, an area with significant free-surface waves was found below the weir, with its length depending on the discharge as well as the weir geometry. With increasing distance from the weir, i.e. at ~15P, this free-surface pattern became smoother for all discharges and geometries. Overall, a similar trend of the free-surface along the domain was observed.

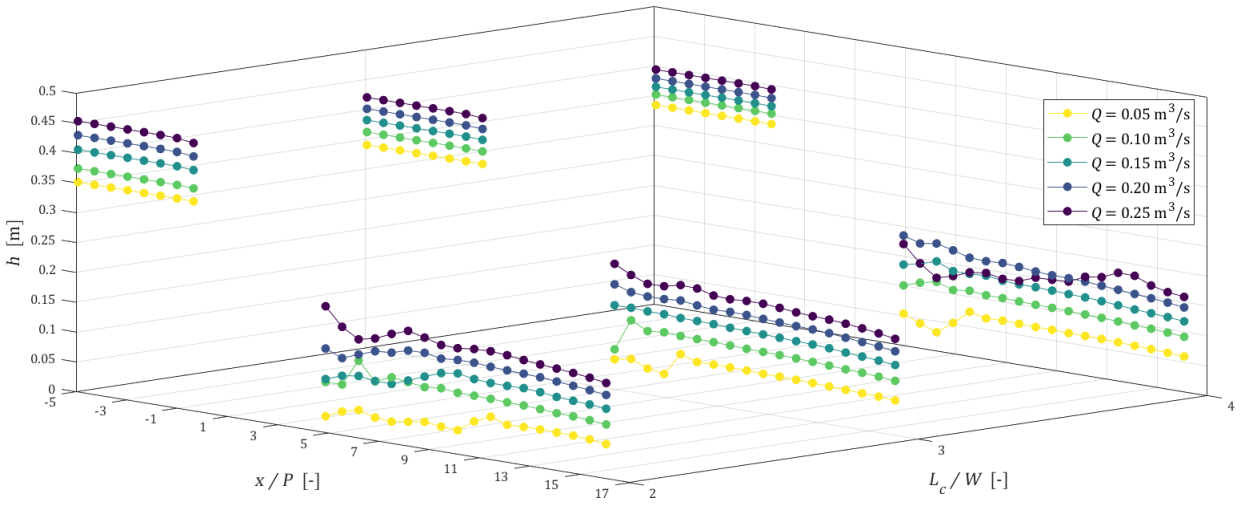

Figure 4. Flow depth (h) along the domain, expressed as a ratio of probe position to weir height (x/P) over all conducted discharges (Q) and geometries (L_c/W).

3.2. Residual Energy

Due to their folded geometry, nonlinear weirs cause a three-dimensional flow field in the outlet cycles and immediately downstream of the weir from nappe collision and thus, more complex energy dissipation processes than linear weirs. Based on laboratory experiments by Magalhaes and Lorena (1994), Lopes et al. (2006) proposed a design equation for estimation of relative residual energy downstream of trapezoidal labyrinth weirs (see. Eq. 1):

$$\frac{H_1}{H_0} = 0.571 + 0.254 \ln\left(\frac{H}{P}\right) + 0.199 \ln\left(\frac{L_c}{W}\right) \quad (1)$$

with H_1 = downstream total head, H_0 = upstream total head and H = upstream head over the weir crest. Eq. (1) was validated by physical model tests for quarter-round crested weirs with $P = 0.25$ m and $1.8 \leq L_c/W \leq 4$ (Lopes et al., 2011, 2008, 2006). The results regarding the residual energy from Lopes et al. (2011) are within the range expected. It is noteworthy that residual energy has been mostly estimated in literature by simple point measurements of flow depth with estimation of kinetic energy by consideration of the continuity equation. However, Carrillo et al. (2020) found notable differences in the velocity profiles depending on probe location downstream of the weir.

In this study, the influence of the three-dimensional downstream flow field on the relative residual energy was investigated. All presented data was extracted after a simulation time of $t = 75$ s, when steady conditions in relation to boundary conditions were obtained. Energy heads were determined as $H = h + U^2/2g$ (with flow depth h, velocity U and gravity acceleration g), accounting for both, depth-averaged (U_{DA}) and section-averaged (U_{SA}) velocities. Furthermore, the kinetic energy correction coefficient α was estimated according to Eq. (2) (with flow area A, sectional mean velocity U_{SA} and local streamwise velocity u). This coefficient was used to describe non-uniform velocity distributions more accurately (Singh et al. (2019). As expected, the coefficient was found to increase close to the weir (see Fig. 5) and to converge to unity further downstream. In detail, the velocity head correction factor was in the range of $1.0003 < \alpha \leq 1.2051$ and thus, was reasonable (Singh et al. 2019; Keshavarzi and Hamidifar 2018; Hulsing et al. 1966).

$$\alpha = \frac{1}{A\, U_{SA}^3} \int_A u^3\, dA \quad (2)$$

Figure 5 illustrates the evolution of the relative residual energy expressed as a ratio of downstream total head H_1 to the upstream total head H_0. H_0 was measured at a fixed distance of -4.92P (-1.5 m). As expected, the positioning of the probes affects the relative residual energy. Near the weir, significant differences between velocity heads from

section-averaged as well as depth-averaged velocity profiles and from local flow depth measurements at the centerline and the continuity equation were observed. With a maximum α of 1.205, the highest influence of α was observed close to the weir as well (see Fig. 5 bottom left). With increasing distance from the weir towards the downstream boundary, a convergence of H_1/H_0 and α was noticed. If the measuring location is far downstream of the structure, a sufficient accuracy can be expected (see Fig. 5). A minimum distance of 15P should be respected for further investigations. At this point, the influence of α was small and can be neglected. Furthermore, a homogeneous progress of H_1/H_0 can be found beyond this minimum distance.

According to this evolution of the flow field, the probe position at 15.42P (4.7 m) was chosen for further comparison. Figure 6 compares selected results with published data from Crookston (2020), Merkel et al. (2018), Lopes et al. (2011, 2008; 2006) and Magalhaes and Lorena (1994). Comparing both velocities U_{DA} and U_{SA}, it was found that the depth-averaged velocity on the flume centerline is generally higher than the section-averaged velocity. Consequently, this fact yields an overestimation of the relative residual energy with depth-averaged data.

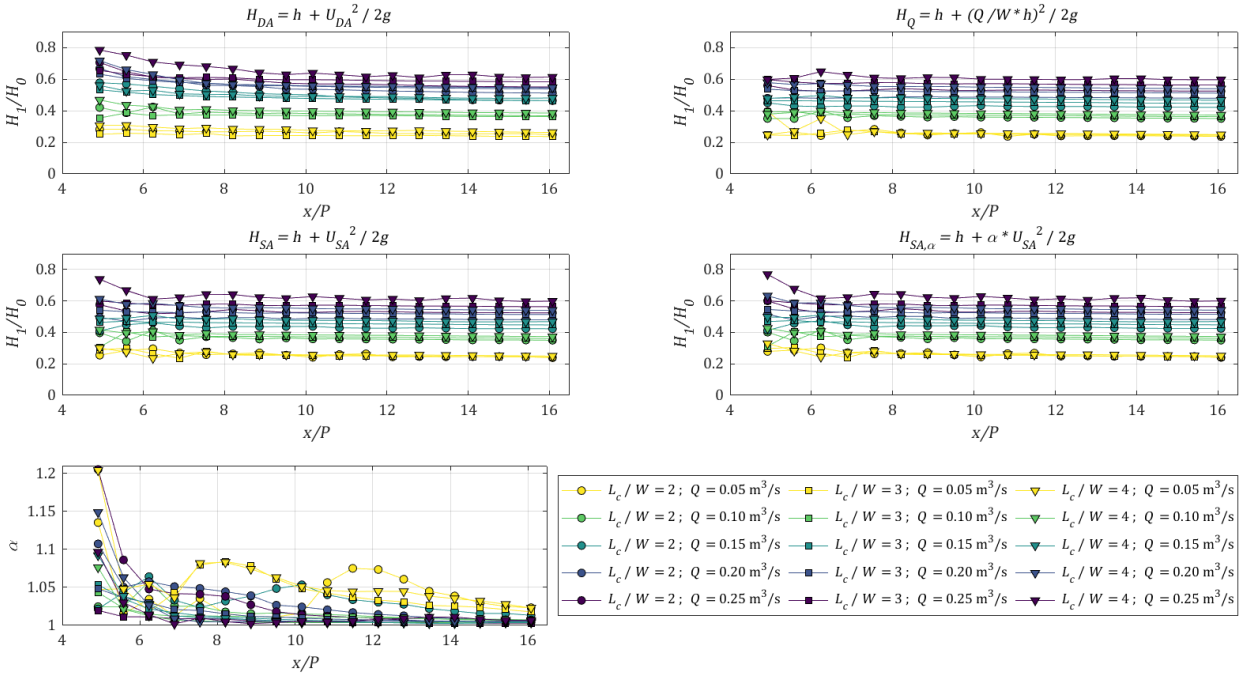

Figure 5. Evolution of relative residual energy along the downstream with different velocity head calculations (H_{DA}, H_Q, H_{SA} and $H_{SA,\alpha}$); evolution of the kinetic energy correction coefficient α along the entire domain.

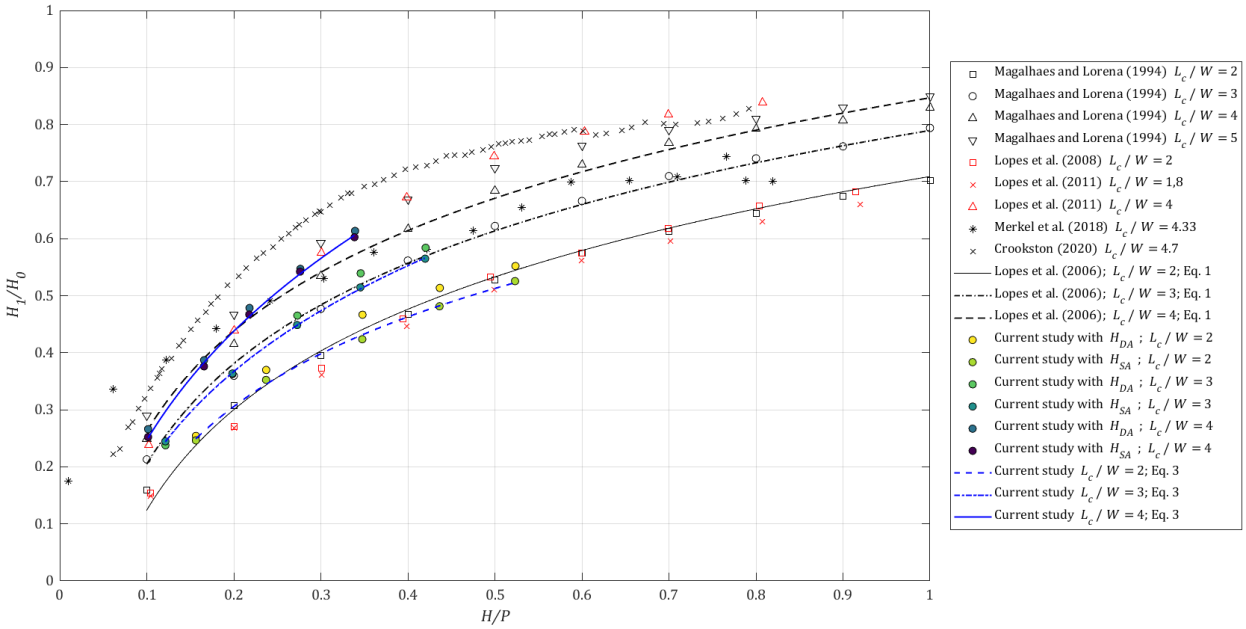

Figure 6. Residual energy of labyrinth weirs from the current study, downstream head estimation with depth-averaged velocities and section-averaged velocities, the kinetic energy correction coefficient α is neglected; rectangular labyrinth weir data from Merkel et al. (2018), trapezoidal labyrinth weir data from Lopes et al. (2011, 2008) and Magalhaes and Lorena (1994).

Besides this overestimation, some differences between simulated and published data are noticeable. They may be caused by the influence of different measuring positions (see Fig. 5), scale effects, different weir heights, sidewall angles, number of cycles or surface tension effects for small headwater ratios. The chosen one fluid approach and the resulting negligence of the air entrainment may have an influence as well. Equation (3) in combination with Table 1 summarizes the presented data of the relative residual energy (see also Fig. 6).

$$\frac{H_1}{H_0} = a\left(\frac{H}{P}\right)^b + c \tag{3}$$

Table 1. Curve-fit coefficients for quarter round trapezoidal labyrinth weirs, presented L_c/W ratios and section averaged velocity heads H_{SA} in Figure 6.

L_c/W	γ [°]	a	b	c	R^2	Validated range
2	26	-6.297	-0.0345	6.926	0.9972	$0.156 < H/P \leq 0.523$
3	16	2.345	0.135	-1.519	0.9998	$0.121 < H/P \leq 0.420$
3	12	1.817	0.244	0.7892	0.9989	$0.102 < H/P \leq 0.339$

4. Discussion and Conclusions

A numerical study of three trapezoidal labyrinth weirs with a constant height of 0.305 m and different ratios of total crest length to total width was conducted. The flume width was 1.22 m. For each geometry, five discharges were studied ($0.05 < Q \leq 0.25$ m^3/s). For the employed mesh resolution, a mean GCI of 9.2% for different parameters was obtained. Some GCI values are higher than the GCI of 10 %, which was recommended by Celik et al. (2008), at small discharges. For the selected cell size, some mesh dependence thus may be present for small discharges and resulting low water levels. Nevertheless, results were found to be generally consistent to literature data for all discharges.

With the conducted simulations, an attempt was made to consider the 3D flow field in the downstream region more precisely. Accordingly, the velocity head was determined with depth-averaged and section-averaged velocities.

Additionally, the kinetic energy correction coefficient α was calculated. A minor influence of this parameter is observed when data is extracted in sufficient distance to the weir where turbulence is reduced and a redirection of the flow is obtained. For further investigations, it is recommended that a minimum distance of 15P is maintained to ensure convergence of H_1/H_0 and α. An empirical design equation is proposed for trapezoidal quarter-round labyrinth weirs. Even though the influence of the crest shape seems to be small, it should not be neglected. Beside the distinction of L_c/W ratios, a further distinction according to crest shape should be made. Furthermore, the presented equation takes the effective velocity profile into account and does not estimate the energy height by using the continuity equation or a depth-averaged velocity. The structure of the presented equation is similar to the equation of the discharge coefficient published by Crookston (2010). In general, high energy dissipation downstream of nonlinear weirs is found in agreement to literature data.

Currently, there is a lack of information regarding laboratory measurements of the described 3D velocity fields. In addition, there are only a few numerical studies on this problem. Future research should focus on extensive 3D laboratory measurements to expand and clarify the existing data basis for more geometries.

5. REFERENCES

Akbari Kheir-Abadi, M., Karami Moghadam, M., Sabzevari, T. and Ghadampour, Z. (2020). "An experimental study of the effects of the parapet walls geometry on the discharge coefficient of trapezoidal piano key weirs." *Flow. Meas. Instrum.,* 73(0955-5986), 101742.

Bayon, A., Valero, D., García-Bartual, R. and Valles-Moran, F. (2016). "Performance assessment of OpenFOAM and FLOW-3D in the numerical modeling of a low reynolds number hydraulic jump." *Environ. Model. Softw.* 80(1364-8152), 322–335.

Ben Said, M. and Ouamane, A. (2022). "Performance of rectangular labyrinth weir – an experimental and numerical study." *Water Supply*, 22(1606-9749), 3628-3644.

Bilhan, O., Cihan Aydin, M., Emin Emiroglu, M. and Miller, C. (2018). "Experimental and CFD analysis of circular labyrinth weirs." *J. Irrig. Drain. Eng.* 144(6), 4018007.

Carrillo, J., Matos, J., and Lopes, R. (2019). "Numerical modeling of free and submerged labyrinth weir flow for a large sidewall angle." *Environ. Fluid Mech.* 20(2020), 357–374.

Carrillo, J., Matos, J. and Lopes, R. (2020). "Numerical modelling of subcritical flow downstream of a labyrinth weir." *Proc.*, *8th IAHR ISHS 2020*. The University of Queensland, QLD., Santiago, Cl., 10.14264/uql.2020.616.

Celik, I., Ghia, U., Roache, P. and Freitas, C. (2008). "Procedure for estimation and reporting of uncertainty due to discretization in CFD applications." *J. Fluids Eng.* 130(7), 078001.

Crookston, B. (2010). Labyrinth weirs. All Graduate Theses and Dissertations. Paper 802. USU Library, Logan, Ga.

Crookston, B. (2020). "A laboratory investigation on residual energy of nonlinear weirs." *Proc., 8th IAHR ISHS 2020.* The University of Queensland, QLD., Santiago, Cl., 10.14264/uql.2020.614.

Crookston, B., Erpicum, S., Tullis, B. and Laugier, F. (2019). "Hydraulics of labyrinth and piano key weirs: 100 years of prototype structures, advancements, and future research needs." *J. Hydraul. Eng.* 145(12), 02519004.

Crookston, B. and Tullis, B. (2012). "Arced labyrinth weirs". *J. Hydraul. Eng.*138(6), 555-562.

Crookston, B., Anderson, R. and Tullis, B. (2018). "Free-flow discharge estimation method for piano key weir geometries." *J. Hydro-Environ. Res.* 19(1570-6443), 160-167.

Dabling, M. and Crookston, B. (2012). "Staged and notched labyrinth weir hydraulics." *Proc., 4th IJREWHS*, USU Library, Logan, Ga. 1-9.

Dabling, M. and Tullis, B. (2017). "Modifying the downstream hydrograph with staged labyrinth weirs." *J. Appl. Water Eng. Res.* 6(3), 183-190.

Erpicum, S., Laugier, F., Boillat, J., Pirotton, M., Reverchon, B. and Schleiss, A. (2011). Labyrinth and Piano Key Weirs – PKW 2011, CRC Press Taylor & Francis Group, London

Erpicum, S., Laugier, F., Pfister, M., Pirotton, M., Guy-Michel, C. and Schleiss, A. (2013). Labyrinth and Piano Key Weirs II – PKW 2013, CRC Press Taylor & Francis Group, London

Erpicum, S., Laugier, F., Ho Ta Khanh, M. and Pfister, M. (2017). Labyrinth and Piano Key Weirs III – PKW 2017, CRC Press Taylor & Francis Group, London.

Falvey, H. (2003). Hydraulic design of labyrinth weirs, ASCE, Reston

Flow Science, Inc. (2020). FLOW-3D HYDRO User Manual, Release 12.0. Santa Fe, Ca.

Ghaderi, A., Daneshfaraz, R., Abbasi, S. and Abraham, J. (2020). "Numerical analysis of the hydraulic characteristics of modified labyrinth weirs." *Int. J. Energ. Water. Res.* 4(2020), 425-436.

Hager, W., Pfister, M. and Tullis, B. (2015). “Labyrinth weirs: developments until 1985.” *Proc., 36th IAHR World Congress*, IAHR, The Hague, NL.
Hay, N. and Taylor, G. (1970). “Performance and design of labyrinth weirs.” *J. Hydraul. Div.* 96(11), 2337–2357.
Hinchliff, D. and Houston, K. (1984). Hydraulic design and application of labyrinth spillways, U. S. Bureau of Reclamation Denver, Co.
Hirt, C. and Nichols, B. (1981). “Volume of fluid (VOF) method for the dynamics of free boundaries.” J. Comput. Phys. 39(1), 201–225.
Hulsing, H., Winchell, S. and Cobb, E. (1966). Velocity-head coefficients in open channels, U.S. G.P.O. Washington, US.
Keshavarzi, A. and Hamidifar, H. (2018). “Kinetic energy and momentum correction coefficients in compound open channels.” *Nat. Hazards* 92(3), 1859–1869.
Lopes, R., Matos, J. and Melo, J. (2008). “Characteristic depths and energy dissipation downstream of a labyrinth weir.” Proc., 2nd IJREWHS, Pisa University Press, Pisa, IT.
Lopes, R., Matos, J. and Melo, J. (2011). “Flow properties and residual energy downstream of labyrinth weirs.” *Proc., Labyrinth and Piano Key Weirs – PKW 2011,* CRC Press Taylor & Francis Group, London, 97–104.
Lopes, R., Matos, J. and Falcao de Melo, J. (2006). “Discharge capacity and residual energy of labyrinth weirs.” *Proc., 1st IJREWHS*, The University of Queensland, Montemor-o-Novo, PT, 47–55.
Magalhães, A. and Lorena, M. (1994). “Perdas de energia do escoamento sobre soleiras em labirinto.” *Proc. 6 SILUSB/1 SILUSBA*, Lisboa, PT, 203-211. (in Portuguese)
Mansoori, A., Erfanian, S. and Khamchin Moghadam, F. (2017). “A study of the conditions of energy dissipation in stepped spillways with Λ-shaped step using FLOW-3D.” *J. Civ. Eng.* 3(10), 856-867.
Merkel, J., Belzner, F., Gebhardt, M. and Thorenz, C. (2018). “Energy dissipation downstream of labyrinth weirs.” *Proc. 7th IAHR ISHS 2018*. USU Library, Logan, Ga., 508-517.
Roache, P. (1994). “Perspective: A method for uniform reporting of grid refinement studies.” *J. Fluids Eng.* 116 (3), 405-413.
Schleiss, A. (2011). “From labyrinth to piano key weirs - A historical review.” *Proc., Labyrinth and Piano Key Weirs – PKW 2011*, CRC Press Taylor & Francis Group, London, 3-15.
Singh, P., Naik, B., Tang, X., Khatua, K., Kumar, A. and Banerjee, S. (2019). “Models for kinetic energy and momentum correction coefficients for non-prismatic compound channels using regression and gene expression programming.” *SN Appl. Sci.* 1(2019), 1229.
Taylor, G. (1968). The performance of labyrinth weirs. PhD thesis, University of Nottingham, Nottingham.
Tullis, B., Willmore, C. and Wolfhope, J. (2005). “Improving performance of low-head labyrinth weirs.” *Proc., Impacts of global climate change. World Water and Environmental Resources Congress 2005*, ASCE, Reston, Va., 1-9.
Tullis, B., Crookston, B., Brislin, J. and Seamons, T. (2020). “Geometric effects on discharge relationships for labyrinth weirs.” *J. Hydraul. Eng.* 146(10), 4020066.
Valero, D., Bung, D. and Crookston, B. (2018). “Energy dissipation of a type III basin under design and adverse conditions for stepped and smooth spillways.” *J. Hydraul. Eng.* 144 (7), 04018036.
Versteeg, H. and Malalasekera, W. (2007). An introduction to computational fluid dynamics. The finite volume method. 2nd ed. Pearson/Prentice Hall, Harlow.
Wilcox, D. (2006). Turbulence modeling for CFD. 3rd Ed., CW Industries, Los Angeles.
Yakhot, V., Orszag, S., Thangam, S., Gatski, T. and Speziale, C. (1992). “Development of turbulence models for shear flows by a double expansion technique.” *Phys. Fluids A, Fluid. Dyn.* 4(7), 1510–1520.